



Anal. Bioanal. Chem. Res., Vol. 11, No. 2, 153-167, April 2024.

Electrochemical Determination of Sunset Yellow in the Presence of Tartrazine by an over Oxidized Poly *p*-Aminophenol Coated Glassy Carbon Electrode Using Experiment Design Method

Beheshteh Ajdari, Tayyebeh Madrakian*, Abbas Afkhami and Mohammad Reza Jalali Sarvestani

Faculty of Chemistry and Petroleum Sciences, Bu-Ali Sina University, Hamedan, 6517838695, Iran

(Received 21 October 2023, Accepted 12 January 2024)

The paper describes a scientific study involving the use of an over-oxidized *p*-aminophenol sensor for the quantification of sunset yellow in the presence of tartrazine. The study utilized the electropolymerization method on a glassy carbon electrode and employed the Box-Benken method to optimize parameters such as pH, step voltage, number of electropolymerization cycles, and precipitation potential. The study assessed the electrode's selectivity towards various ionic species and found no significant interference. It determined a linear range between 0.25 and 300.0 μM for sunset yellow, with a detection limit of 0.09 μM . The electrode modified with PAP-OX underwent assessments of repeatability and reproducibility, yielding relative standard deviation (RSD) values of 1.14% and 4.09%, respectively. The primary objective of the research was to quantify the concentration of Sunset Yellow in different food samples, including ice cream, fruit juice, powdered jelly, Smarties, and chocolate, while considering the presence of tartrazine. Overall, the study focused on developing a sensor for the quantification of sunset yellow in food and drink samples, with a particular emphasis on optimizing the sensor's performance and assessing its reliability for practical applications.

Keywords: Over-oxidized *p*-aminophenol, Sunset yellow, Experimental design, Glassy carbon electrode

INTRODUCTION

Artificial colors have been the top choice in the food industry for many years due to their stability against light, oxygen, and pH, as well as lower levels of microbiological contamination [1]. Azo dyes, which contain the azo group (-N=N-), are widely used in various industries including food, pharmaceuticals, cosmetics, and textiles [2]. Two commonly used azo dyes in food coloring are Sunset Yellow (SY) and Tartrazine (TZ), known for their ability to maintain color and enhance texture in a variety of food and beverage products. The simultaneous presence of SY and TZ is essential for achieving the desired yellow color in food products [3]. However, despite their beneficial properties, these colors may have potential negative impacts on human

health due to their chemical structure [4]. Azo dyes with an azo functional group (N=N) and aromatic ring structure can be found in everyday consumables such as soft drinks, snacks, ice cream, candy, yogurt, gelatin, chips, pickles, pudding, honey, mustard, and chewing gum [5]. To address the determination of SY and TZ in food products and their potential health impacts, the analysis is conducted on their coexistence [6]. Electrochemical methods offer a compelling option for analyzing these food colors due to the electrochemical activity of SY and TZ, allowing for their direct identification using a redox signal. In conclusion, while artificial colors like SY and TZ provide stability and enhance the visual appeal of food products, their potential health risks should be carefully considered [7]. The use of electrochemical methods for analyzing these colors can provide valuable insights into their presence and concentration in food items, contributing to informed

*Corresponding author. E-mail: madrakian@basu.ac.ir

decision-making in the food industry. Although food dyes like SY and TZ are commonly used in many countries, excessive and uncontrolled consumption of these dyes can lead to a range of health issues such as asthma, autism, allergies, hyperactivity in children, immune system suppression, eczema, anxiety, migraines, and even cancer [8-10]. In response to these risks, several European countries have banned the use of SY coloring due to its carcinogenic properties, although it remains legal in some countries [11]. The European Food Safety Authority (EFSA) has strict regulations for azo dye levels in food and beverages, aiming to protect consumers from potential health risks. The maximum levels vary by product type, such as 50 mg/L for non-alcoholic drinks and 500 mg/kg for food decorations, coatings, and sauces. Additionally, EFSA has set Acceptable Daily Intake (ADI) levels for specific azo dyes to prevent excessive daily exposure and minimize health risks. These regulations are essential for ensuring the safety of food and beverage products [12-14]. The European University Association has also prohibited the use of these dyes due to concerns about their potential negative effects on human health. Given the potential health risks associated with food additives like SY and TZ, accurate measurement of these substances is crucial [15]. In recent years, electrochemical methods have emerged as a popular technique for detecting food colors due to their high specificity, simplicity, low cost, short analysis time, and portability compared to other methods like High-Performance Liquid Chromatography (HPLC) [16], capillary electrophoresis (CE) [17], spectrophotometry [18], Surface Enhanced Raman Scattering (SERS) [19], fluorescence resonance energy transfer [20] and Fluorescence emission spectroscopy [21]. Most of these techniques involve the oxidation of either the hydroxyl group of the Pyrazole TZ ring or the Hydroxyl group of the SY Naphthalene group [22]. However, only a few studies have explored the reduction of the diazonium group due to interference from dissolved oxygen and selection issues. Polymeric materials that can conduct electricity, such as Polyaniline (PANI), Polypyrrole (PPy), Polyazulene, Polyfluorene, Polythiophene, and Polyaminonaphthalenes, exhibit distinct electrical and physical characteristics that enable their application in various fields, including batteries [23], supercapacitors [23], electrochromic devices [24], sensors [25], solar cells [26], and biomedical [27]

applications. Polyaminophenols are a class of conducting polymers that have garnered significant attention due to their unique properties. These polymers contain amine and phenol functional groups, which provide a greater number of active sites for interaction with analytes on the surface of synthesized polymer films compared to other polymers [28]. In particular, poly p-aminophenol demonstrates high stability, excellent conductivity, and electrocatalytic properties, making it a promising candidate for various applications. One notable characteristic of poly p-aminophenol is its ability to enhance the number of defects and conductivity of the electro-synthesized polymer film when oxidized. This property further contributes to its appeal for a wide range of applications [29]. Overall, the exceptional stability, conductivity, and electrocatalytic properties of poly p-aminophenol make it an attractive option for diverse applications in fields such as sensing, energy storage, and electrochemical devices. Its unique combination of functional groups and enhanced properties sets it apart as a valuable material for future technological advancements. [30].

In recent times, chemometric techniques have gained widespread popularity for optimizing analytical methods, primarily owing to their capacity to minimize the number of experiments needed, thereby leading to reduced laboratory work and lowered expenses on reagents [31]. The first step in this optimization process is often to use a Plackett-Burman design (PBD) to screen experimental factors and identify significant variables affecting the method's efficiency. PBD is a type of screening experiment that is particularly useful when there are too many factors to test in-depth. Its purpose is not to create an exhaustive model but rather to identify the primary factors affecting the experiment. After identifying the factors, a Box-Behnken design (BBD) can be utilized to optimize them [32]. The BBD is recognized as one of the most robust response surface designs, possessing the ability to qualify the quadratic model, detect a lack of fit, utilize blocks, and construct sequential designs. It requires fewer experimental runs than other methods and allows for specific positioning of design points [33,34].

This research aimed to synthesize electropolymerization PAP-OX and evaluate its electrocatalytic properties in the electro-oxidation of SY. Subsequently, experimental parameters were optimized using BBD methodology, and the

effectiveness of PAP-OX as an electrode modifier for detecting SY in the presence of TZ in food samples was examined.

MATERIALS AND METHODS

Chemicals and Apparatus

The chemical composition of SY and TZ is illustrated in Fig. 1. For the experiment, all materials including SY and TZ, Sodium Dodecyl Sulfate (SDS), Sodium Hydroxide (NaOH), Sulfuric Acid (H₂SO₄), Alumina (Al₂O₃), Ethanol, Acetic Acid (CH₃COOH), Boric Acid (BH₃O₃), Phosphoric Acid (H₃PO₄), and Hydrochloric Acid (HCl) were procured from Merck Company (Darmstadt, Germany) or Sigma Aldrich Company (USA) without any prior purification. All the stock solutions were utilized in Double Distilled Water (DDW). In order to support the electrolyte, a 5.0 mM solution of Britton Robinson Buffer (BRB) with a pH of 9.0, which was adjusted using NaOH, was used for all the voltammetric experiments. To prepare BRB, a solution containing 0.04 M of acetate acid, boric acid, and phosphoric acid was mixed with a soda solution to adjust the pH level. All voltammetric analyses were carried out utilizing the Metrohm 797 VA Computrace Polarograph. To adjust the pH levels of the solutions, a combined glass electrode and a Metrohm 827 pH meter (Herisau, Switzerland) were used. The glassy carbon electrode (GCE), Ag/AgCl (saturated KCl) reference electrode, and Pt electrode counter electrode used during the experiment were procured from Azar Electrode Company located in Urmia, Iran. The Auto lab PGSTAT 302 N model potentiostat/galvanostat, manufactured by Eco-Chemie in the Netherlands, was utilized to perform Electrochemical impedance spectroscopy (EIS), with NOVA 1.11 software used for the purpose.

Fabrication of Modified Electrode

The glassy carbon electrode was first polished for 120.0 s using an alumina slurry with a particle size of 0.4 μm. Subsequently, the electrode was soaked in an ultrasonic bath containing a mixture of DDW and Ethanol with a 1:1 ratio for a period of 10.0 min to prepare it for electrochemical polymerization. To initiate the polymerization process, the electrode was submerged in a solution comprising 7.0 mM SDS, 50.0 mM *p*-Aminophenol, and 1 mM HCl.

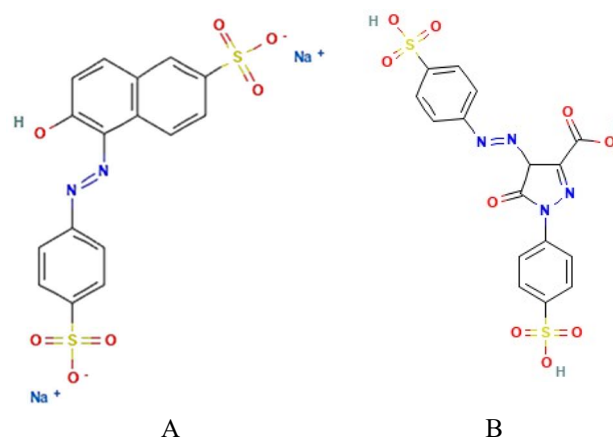


Fig. 1. Chemical structure of food colors: A; Sunset yellow, B; Tartrazine

Subsequently, cyclic voltammetry was carried out by applying 15.0 repetitive potential cycles ranging from -0.645 to 1.955 V vs. Ag/AgCl at a scan rate of 100.0 mV s⁻¹. To improve the conductivity and porosity of the PAP/GCE, the modified electrode was subjected to over-oxidation for 360.0 s in a 0.1 M NaOH solution at +1.2 V, resulting in the modified electrode being referred to as PAP-OX /GCE. The final step included cleaning the PAP-OX/GCE modified electrode using DDW.

Experimental Procedure

In order to obtain a consistent and reproducible response, the modified electrode was subjected to cyclic voltammetry within the range of 0.5-1.2 V, with a sweep rate of 25 mV s⁻¹ in the supporting electrolyte of BRB for three cycles before each voltammetric measurement. This preparatory process was implemented to ensure that the electrode was appropriately conditioned and that the outcomes obtained were reliable and consistent. The electrochemical experiments, namely square wave anodic stripping voltammetry (SWAVS) and cyclic voltammogram (CV), were conducted according to standard protocols involving an initial accumulation period of 60 s at -0.35 V. The SWAVS experimental parameters included a pulse amplitude of 30 mV, a frequency of 50 Hz, and a phase voltage of 3 mV.

Real sample Preparation

The study selected various real samples suspected to

contain SY and TZ, including jelly powder, soda, ice cream, stone chocolate, smarties, and fruit juice, which were purchased from a local supermarket in Hamedan City. For solid samples like jelly powder, smarties, and rock chocolate, homogenization was first performed, followed by weighing 5.0 mg and dissolving in 10.0 ml of DDW using ultrasonication. The solution was then centrifuged at a speed of 4000 rpm and filtered through Whatman 0.4 mm filter paper. Subsequently, 1.0 ml of this solution was diluted 200.0 times with Britton-Robinson buffer adjusted to pH 9.0 for analysis. Liquid samples such as fruit juice were also centrifuged at a speed of 4000 rpm, and the supernatant was filtered. 1.0 ml of this solution was then diluted 200.0 times with Britton Robinson buffer, and 5.0 ml was used for analysis. On the other hand, the soft drink sample was degassed using an ultrasonic for 30.0 min, followed by centrifugation, filtering, dilution, and analysis[5,35-37].

RESULTS AND DISCUSSION

Electrochemical characterization of PAP-OX/GCE

As depicted in Fig. 2, the process of electropolymerization, utilized to generate poly(*p*-aminophenol), features a CV indicating an irreversible oxidation peak at 1.56 V *vs.* Ag/AgCl. Conversely, the voltammogram demonstrates quasi-reversible reduction and oxidation peaks at 0.67 V and 0.31 V *vs.* Ag/AgCl, correspondingly, for *p*-aminophenol. When subjected to negative potential values and an increased number of voltammogram cycles, a considerable quantity of polymer is produced on the electrode surface [38]. As Fig. 2 shows, the anodic peak current at 1.56 V gradually decreases while the cathodic peak increases at +0.67 and +0.31 V [39]. CV was performed at a scan rate of 100 mV s⁻¹ with a cycle number of 15 and an over-oxide time of 360 s. To improve the modified electrode's porosity and conductivity with poly-*p*-aminophenol, it is subjected to oxidation in a 0.1 M NaOH solution at a potential of 1.2 V *vs.* Ag/AgCl for 360 s [40].

In order to examine the prepared PAP-OX/GCE, initial experiments were conducted. The present study evaluated the electro-catalytic activity of PAP-OX/GCE and optimized the experimental conditions for determining SY in the presence of TZ using PAP-OX modified electrode. Additionally, the modified electrode using PAP-OX was utilized in these experiments, and the obtained outcomes are elaborated in this report.

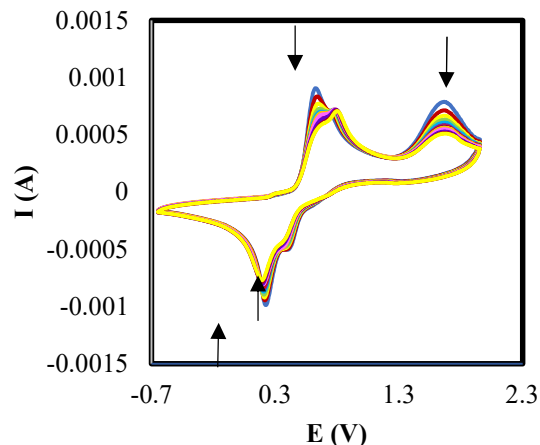


Fig. 2. CV of *p*-aminophenol electropolymerization in a 5.0 mM *p*-aminophenol monomer in 1.0 M HCl solution on a GCE in the presence of 5.0 mmol SDS at a scan rate of 100 mV s⁻¹. The arrows indicate the trends of current during CVs.

The study employed two electrochemical techniques, namely cyclic voltammetry and square wave voltammetry. Figure 3 displays SWAVS and CV for SY in the presence of TZ. Figure 3a presents the electrochemical response of a GCE modified with PAP-OX. The voltammogram shows an oxidation peak occurring at 0.786 V and a corresponding cathodic peak at 0.761 V *vs.* Ag/AgCl. The measured difference between the cathodic and anodic peak potentials for SY was found to be 25 mV. On the other hand, a distinct irreversible electrode reaction was observed for TZ at a potential of 1.048 V *vs.* Ag/AgCl. These findings suggest that SY undergoes a reversible redox reaction, while TZ experiences irreversible oxidation when interacting with the proposed voltammetric platform.

The square wave voltammetric technique was also employed to study the electrochemical behavior of SY in the presence of TZ. Figure 3b provides a visual representation of the SWASV for 5 μM SY and 10 μM TZ in a pH 9.0 BRB solution. The voltammogram shows a well-defined anodic peak at 0.716 V for SY and a weak anodic peak at 0.93 V for TZ. This indicates that the sensitivity of the electrode toward SY is more than that for TZ and their peaks do not overlap when they are in the mixture in the sample even when the concentration of TZ is more excess over SY. Therefore, the electrode can be used for the determination of SY in the presence of excess amounts of TZ.

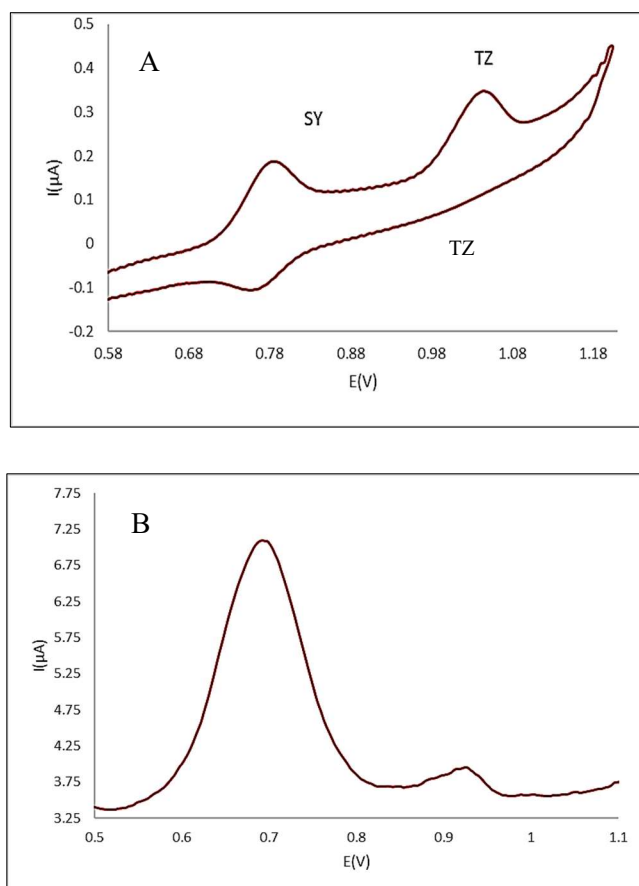


Fig. 3. A) CV and B) SWASV for the solution containing a mixture of 5 μM SY and 10 μM TZ in BRB (pH 9.0) at PAP-OX/GCE.

The SWASV for 5.0 μM solution of SY at glassy carbon bare electrode (GCE), on the PAP-modified GCE, and PAP-OX-modified GCE in BRB solution of pH 9 was recorded. The results are shown in Fig. 4. The results revealed a significantly low current intensity at the bare electrode compared to the modified electrodes. A higher current intensity of about 24.37 times was observed at the PAP-OX electrode than at the PAP-modified electrode, indicating better sensitivity in the oxidized state. This may be due to the higher surface area of the PAP-OX-modified electrode. Moreover, the PAP-OX-modified electrode displayed a shift towards less positive anodic potential compared to the PAP-modified electrode, making the reduction process easier in the modified electrode due to the electrocatalytic effect of the PAP-OX surface.

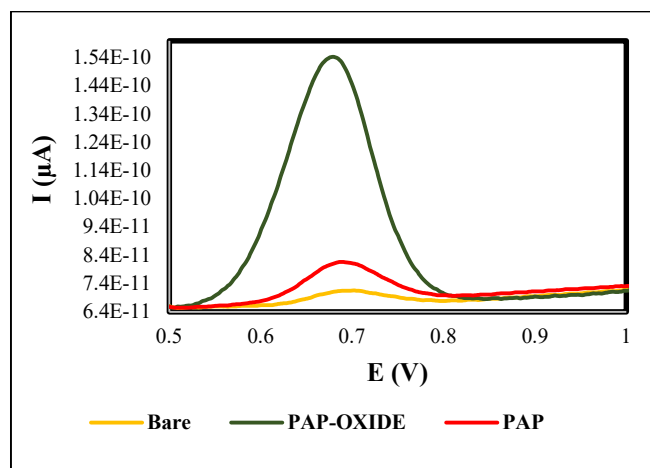


Fig. 4. SWASV of a 5.0 μM solution of SY in BRB (pH = 9.0) on the surface of bare GCE (a), PAP/GCE (b), and PAP-OX/GCE (c).

The performance of the electrochemical sensor is influenced by the physical characteristics of the electrode surface. Upon subjecting the PAP film to high substrate potential during oxidation, there is an alteration in the coating.

Our previous investigations indicated that the over-oxidized surface is a non-uniform layer that is swollen and characterized by sizable spherical particles that are randomly dispersed and covered enveloping the electrode surface. This configuration results in a higher level of porosity when compared to the glassy carbon electrode coated with PAP [39]. On the electro-synthesized polymer film before and after the over-oxidation process (referred to as PAP and PAP-OX films). FT-IR spectroscopy studies showed that upon over-oxidation of PAP, a variety of nitrogen and oxygen-containing functional groups, such as carbonyl and amine groups, are formed on the surface of the modified electrode. These newly generated functional groups facilitate enhanced interaction between the analyte and the electrode surface through hydrogen bonding [40].

Electrochemical Impedance Spectroscopy (EIS)

Electrochemical impedance spectroscopy (EIS) is an effective technique for studying the interfacial properties of modified electrodes [41]. The process of modifying the electrode surface through the use of polyelectrolytes,

surfactants, conductive polymers, nanomaterials, or semi-conductive materials brings about significant alterations in the capacitance of the two layers and the surface electron transfer resistance of the electrode. Figure 5 depicts the Nyquist diagrams of $\text{Fe}(\text{CN})_6^{3-/4-}$ on various electrodes, including bare GCE (colored Orange), PAP GCE (colored Violet), and PAP-OX/GCE (colored Red). The diameter of the semicircle observed at high frequencies in the Nyquist diagram indicates the electron transfer resistance (R_{ct}), while the linear section observed at low frequencies is typically associated with the diffusion process. Moreover, the R_{ct} values of Bare (Orange) and PAP-OX GCE (Red) were also observed. The application of a PAP-OX film to the GC surface leads to a significant decrease in the R_{ct} value. According to the results, the modified electrode surface displayed decreased resistance to the redox process of the probe pair in comparison to the unmodified GC surface. Moreover, the disparity in the R_{ct} values between the bare and modified electrodes indicated the formation of a PAP-OX layer on the surface after the modification process. The experimental setup, as depicted in Fig. 4, includes an equivalent circuit comprising various components. These components consist of R_1 , representing the solution resistance, W_s the Warburg impedance, CPE representing the constant phase element, and R_2 , which denotes the charge transfer resistance [42]. The impedance data obtained from the insertion in Figure 4 led to the selection of the Randles circuit for fitting. The value of R_2 , which depends on the dielectric and insulating properties of the electrode/electrolyte interface, was estimated to be 558Ω at the GCE (a). However, the acceleration of electron transfer by PAP resulted in a decrease in R_2 to 502Ω (b). By using the PAP-OX/GCE, the R_2 decreased further to 248Ω (c), indicating that the electron transfer resistance on the PAP-OX/GCE was significantly lower compared to that on the PAP/GCE. These findings suggest that successful modification of oxidation occurred at the surface of the PAP/GCE, leading to a substantial improvement in conductivity.

Optimization of Effective Operational Parameters by Experimental Design

Optimization parameters. Several parameters were targeted for optimization in this study, including deposition

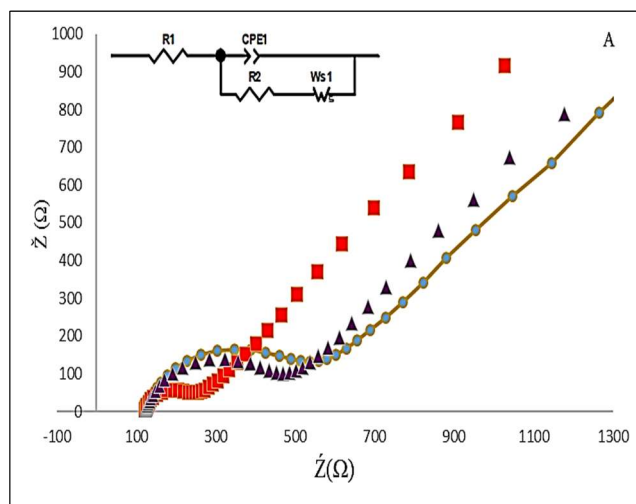


Fig. 5. EIS for Bare GC (colored Orange), PAP GCE (colored Violet), and PAP-OX/GCE (colored Red) and in 1.0 M $[\text{Fe}(\text{CN})_6]^{3-/4-}$ containing 0.1 M KCl.

potential, deposition time, pH, frequency, voltage step, pulse amplitude, Number of cycles, and over-oxidation time. The study employed a PBD as the initial screening method to identify all the influential factors after identifying the significant variables; they were optimized using the BBD in the next phase of the study. To carry out both the BBD and PBD in this study, version 18.0 of MINITAB software was utilized.

Screening of variables using PBD. An ANOVA analysis was conducted to assess the efficacy of PBD in relation to the response Y_1 , and the outcomes are outlined in Table 1. The p-value in the ANOVA table is a useful tool for assessing the significance of each coefficient and can indicate the strength of interaction between independent variables [43]. A p-value below 0.05 suggests that the model terms are significant. Table 1 displays a significant F value of 49.13 and a p-value of 0.004, which indicates that the model is statistically significant. The Pareto chart, which is a valuable tool for identifying the most important effects [44], was also used to determine the significant factors, as shown in Fig. 5 [45]. The ANOVA effect estimates are ranked by absolute value on this chart, with each effect's magnitude represented by a column. Often, a line across the columns indicates the minimum size required for an effect to be statistically significant, as illustrated in Fig. 6 [46].

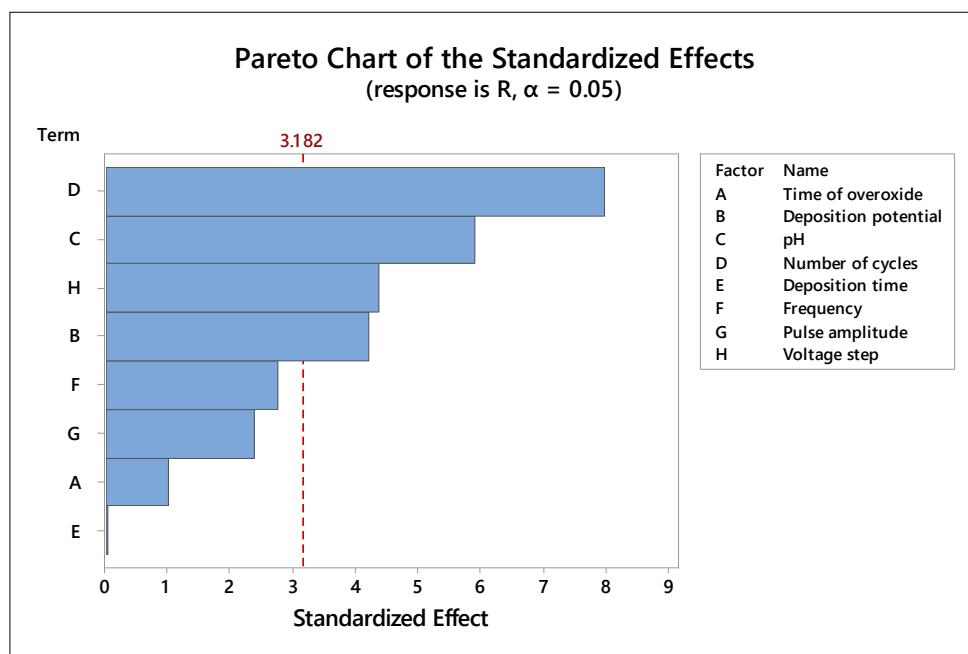


Fig. 6. The Pareto chart.

Table 1. Analysis of Variance (ANOVA) for the Regression Model Using the PBD

Source	DF	Adj SS	Adj MS	F-Value	P-Value
Model	8	1776.59	222.074	49.13	0.004
Linear	8	1776.59	222.074	49.13	0.004
Overoxidizing time	1	0.94	0.941	0.21	0.679
Deposition potential	1	146.72	146.720	32.46	0.011
pH	1	497.68	497.683	110.10	0.002
Number of cycles	1	718.58	718.582	158.97	0.001
Deposition time	1	0.31	0.307	0.07	0.811
Frequency	1	49.78	49.776	11.01	0.045
Pulse amplitude	1	44.31	44.314	9.80	0.052
Voltage step	1	318.27	318.270	70.41	0.004
Error	3	13.56	4.520		
Total	11	1790.15			

As well as the Pareto chart revealed that the number of cycles (X_1), pH (X_2), deposition potential (X_3), and voltage step (X_4) all had a significant impact on the SWASV peak current response intensity at the 5% level ($P = 0.05$). The equation for four factors is stated as follows:

$$R = -146.0 + 4.096 X_1 + 25.27 X_2 + 11.13 X_4 - 90.5 X_3 - 0.01657 X_1 X_1 - 1.454 X_2 X_2 - 0.575 X_4 X_4 - 144.0 X_3 X_3 - 0.2259 X_1 X_2 - 0.2650 X_1 X_4 + 4.513 X_1 X_3 - 0.206 X_2 X_4 - 13.16 X_2 X_3 + 5.17 X_4 X_3$$

Optimization parameters by BBD. The study aimed to optimize the four critical factors, namely Number of cycles (X_1), pH (X_2), deposition potential (X_3), and voltage step (X_4) using a BBD. The decision to use BBD was made based on the information obtained from PBD. In this experiment, 27 tests were carried out to examine the effects of the four primary independent variables on peak current response. Three repetitions of the center point were also performed to assess the reproducibility of the outcomes. The experiments were conducted in duplicate, and regression analysis was utilized to calculate the response function coefficients using the experimental data.

Statistical analysis. Table 2 displays the outcomes of ANOVA, which illustrate that for both the number of cycles (X_1) and pH (X_2) factors, the p-values are less than 0.05 (0.000 and 0.000, respectively). These results suggest that the number of cycles (X_1) and pH (X_2) factors play a crucial role in enhancing the SWASV peak current response. On the other hand, the p-values for voltage step (X_4) and deposition potential (X_3) are 0.116 and 0.701, respectively. These values suggest that these two factors do not have a significant impact on the resulting current response[47].

The effectiveness of the quadratic polynomial model was assessed by measuring the coefficient of determination, R^2 .

Table 2. ANOVA for BBD

Source	DF	Adj SS	Adj MS	F-Value	P-Value
Model	14	2264.70	161.76	46.96	0.000
Linear	4	1619.61	404.90	117.55	0.000
X_1	1	153.01	153.01	44.42	0.000
X_2	1	1456.18	1456.18	422.77	0.000
X_4	1	9.88	9.88	2.87	0.116
X_3	1	0.53	0.53	0.15	0.701
Square	4	193.12	48.28	14.02	0.000
$X_1 * X_1$	1	14.64	14.64	4.25	0.062
$X_2 * X_2$	1	180.45	180.45	52.39	0.000
$X_4 * X_4$	1	28.25	28.25	8.20	0.014
$X_3 * X_3$	1	55.96	55.96	16.25	0.002
2-Way Interaction	6	451.97	75.33	21.87	0.000
$X_1 * X_2$	1	81.63	81.63	23.70	0.000
$X_1 * X_4$	1	112.36	112.36	32.62	0.000
$X_1 * X_3$	1	183.33	183.33	53.23	0.000
$X_2 * X_4$	1	2.71	2.71	0.79	0.393
$X_2 * X_3$	1	62.33	62.33	18.10	0.001
$X_4 * X_3$	1	9.61	9.61	2.79	0.121
Error	12	41.33	3.44		
Lack-of-Fit	10	39.89	3.99	5.51	0.163
Pure Error	2	1.45	0.72		
Total	26	2306.03			

$R^2 = 0.9821$; Adjusted $R^2 = 0.9722$; Predicted $R^2 = 0.8788$; 95% significant level.

he R^2 , R^2 -adjusted, and R^2 -predicted values were found to be 0.9821, 0.9722, and 0.8788, respectively. These values suggest a strong correlation between the experimental and theoretical results. To achieve a good fit for a model, Joglekar and May [48] recommend that the R^2 value should be equal to or greater than 0.80. Based on the lack of fit p-value of 0.163, it can be concluded that the analysis is not statistically significant in terms of pure error.

According to Table 2, the p-values for the interaction between factors (X_1X_1 , X_2X_3 , and X_3X_4) are above 0.05, indicating that these factors are insignificant. The impact of four significant variables on peak current was evaluated using response surface methodology and the Box-Behnken

model. To investigate the correlation between the response and factors, surface plots were utilized while keeping the remaining factors constant at specific levels. The article presents an evaluation of the influence of process variables on peak current, detailing their individual effects. The interaction between the factors is illustrated in Fig. 7. The existence of interaction among the factors suggests that they may have a combined impact on the response instead of acting independently. As a result, their collective effect can be more significant or less significant than what would be expected if their individual effects were merely added together [49].

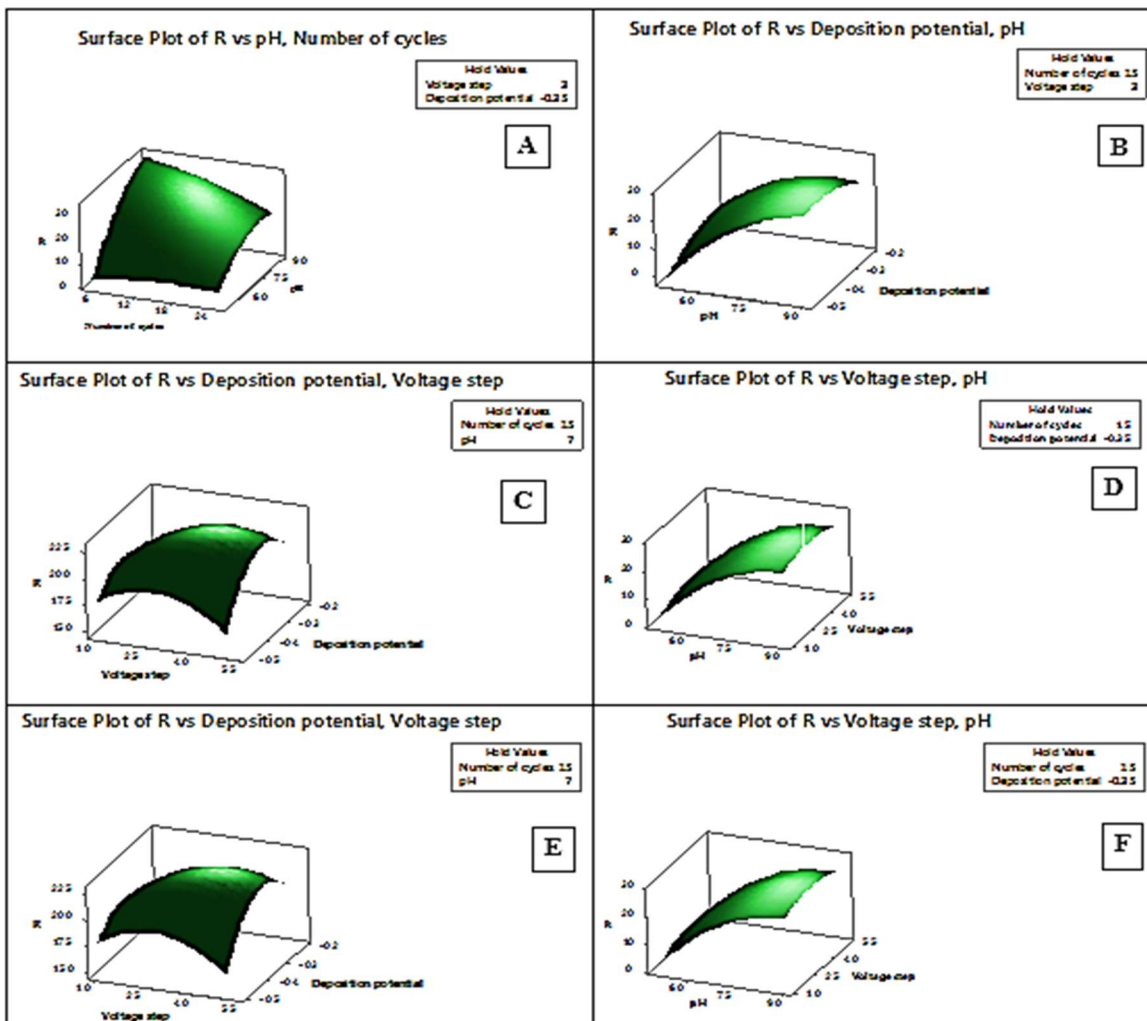


Fig. 7. Response surface plots showing the influence of the Number of cycles, pH, deposition potential, and voltage step and deposition potential.

The important experimental parameters, including pH, voltage step, deposition potential, and number of cycles, were optimized using the utility method to achieve optimal values and maximum response of the peak current. These optimization techniques aimed to maximize the peak current response of SY using the square wave voltammetry method. Based on the results of regression analysis, the optimized values for these factors are pH = 9.0, voltage step = 3.0 mV, deposition potential = -0.35, and number of cycles = 15.

The optimal number of electropolymerization cycles was determined in order to achieve the best measurement conditions. The sensor's conductivity increased with the increasing number of cycles, reaching a peak at 15 cycles. While increasing the number of cycles, the electrode surface eventually becomes obstructed, leading to a decline in the electrode's conductivity.

The mechanism of SY oxidation at the modified electrode was investigated by studying the behavior of peak potential using SWASV and CV at various pH levels ranging from 5 to 9 in the BRB carrier electrolyte. The CV voltammograms of SY in $5 < \text{pH} < 9$ is shown in Fig. 8. By varying the maximum electric currents and peak potentials, we can observe that the pH level of the electrolyte solution greatly affects the oxidation of SY at PAP-OX /GCE. By elevating the pH level from 5.0 to 9.0, the oxidation peak currents (Fig. 8A) of SY exhibit a gradual increase when tested on PAP-OX-modified GCE. Notably, the oxidation signal of SY demonstrates a high sensitivity in a pH 9.0 buffer. Moreover, the influence of pH value on the oxidation peak potential was investigated. It was observed that the oxidation peak potential progressively shifts towards the less positive potentials as the pH value increased from 5.0 to 9.0, indicating the involvement of protons in the oxidation process of SY [6].

As Fig. 1 shows, SY possesses a structural composition consisting of a sulfuric acid functional group, a naphthalene ring, and an azo group. The oxidation mechanism of SY involves the exchange of protons with electrons. Under the influence of pH 9, the azo group undergoes deprotonation, resulting in a decrease in current intensity [50]. Additionally, there is a linear relationship between the anodic peak potential, which is approximately equal to half of 60 mV (Fig. 8B)[51] that is relevant to the transfer of two electrons and one proton for the electro-oxidation mechanism of Sunset Yellow [4].

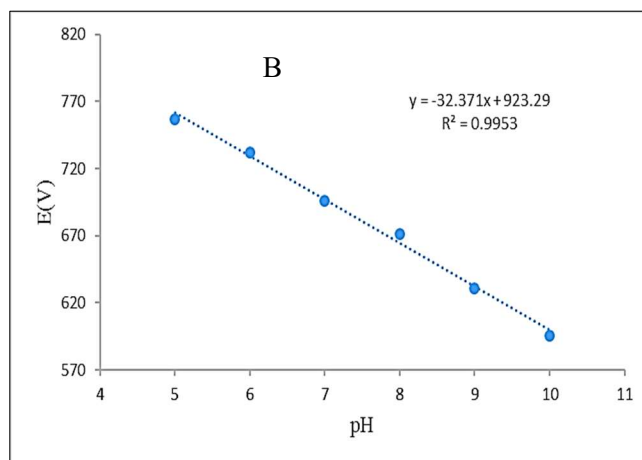


Fig. 8. pH SY (A) CV of SY 5 μM with scan rate 25 in pH 5.0 to 9.0 (B) plot of potential peak (E_{pa}) as a function of solution pH.

Electrochemical Behavior of SY on a Modified Electrode

The electrochemical behavior of SY was assessed through CV analysis conducted in BRB with a pH of 9.0 and a potential range of 0.5 to 1.2 V at various scan rates ranging from 0.04 to 0.55 V s^{-1} . The anodic and cathodic peaks current of SY exhibited a linear increase with the rise in scan rate, suggesting that the surface adsorption controls the process. The equation for the relationship between scan rate and anodic and cathodic peaks current is $I_{\text{pa}} = 12.12v - 0.3812$ ($R^2 = 0.9965$), $I_{\text{pc}} = -9.9386v + 0.1122$ ($R^2 = 0.9914$) which confirms the process of surface adsorption. The SY redox peaks exhibited minimal shift with scan rate variation, indicating that the PAP-OX/GCE redox process is reversible.

Calibration Curve

Under the specified favorable conditions, the SWASV method was employed to accurately measure SY in the presence of TZ. A calibration curve was established by conducting at least three repeated measurements on average (refer to Fig. 10). It was observed that the peak current exhibited a linear increase corresponding to an increase in concentration ranging from 0.25 to 300.0 μM . The concentration of SY (CSY) and the peak current showed a linear correlation, which can be described by two linear equations: $I (\mu\text{A}) = 5.8407 C_{\text{SY}} (\mu\text{M}) + 1.5535$ ($R^2 = 0.9935$)

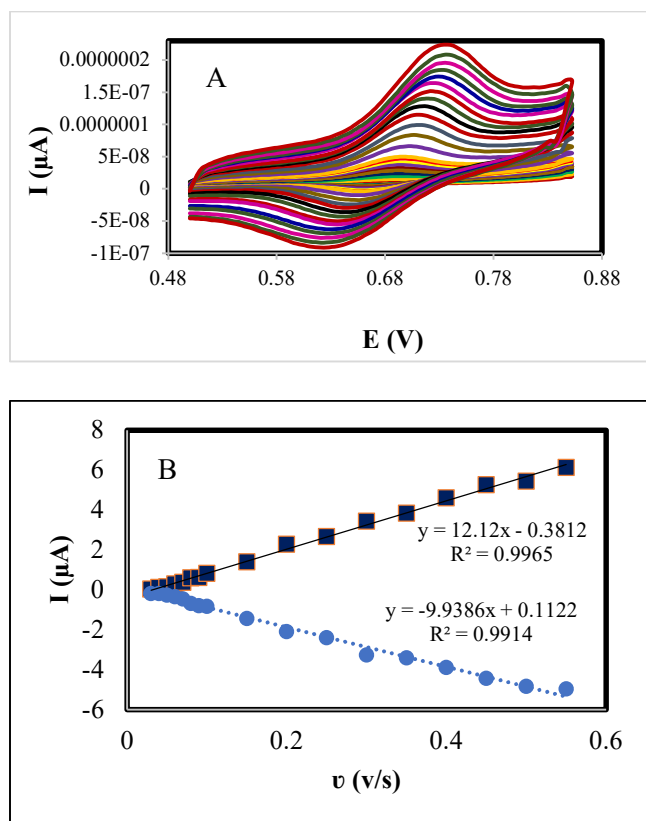


Fig. 9. (A), CVs of 5.0 μM SY on the OX-PAP/GCE at various scan rates (0.04 to 0.55 V s^{-1}) in BRB (pH 9.0) (B) variation of I_{pc} and I_{pa} vs. v (V s^{-1}).

for the concentration range of 0.25 to 5.00 μM , and I (μA) = $0.165 C_{\text{SY}} (\mu\text{mol}) + 28.53$ ($R^2 = 0.9943$) for the concentration range of 5.00 to 300.00 μM .

In the lower concentration range (0.25–5 μM), it appears that the analyte adheres to the surface of the electrode through an adsorption mechanism. This conclusion is supported by the significantly higher slope (5.84) observed within this range. However, in the second dynamic range (5–300 μM), the diffusion mechanism becomes dominant, resulting in a noticeable decrease in slope to 0.165. The limit of detection (LOD), determined using the IUPAC ($3S_b/m$) method, was estimated to be 0.09 μM .

The PAP-OX/GCE sensor's performance was compared with that of other modified electrodes used in literature to determine SY. Table 3 was utilized to display the electrochemical technique type, linear concentration range, LOD value, electrode type, electrode lifetime, and simplicity

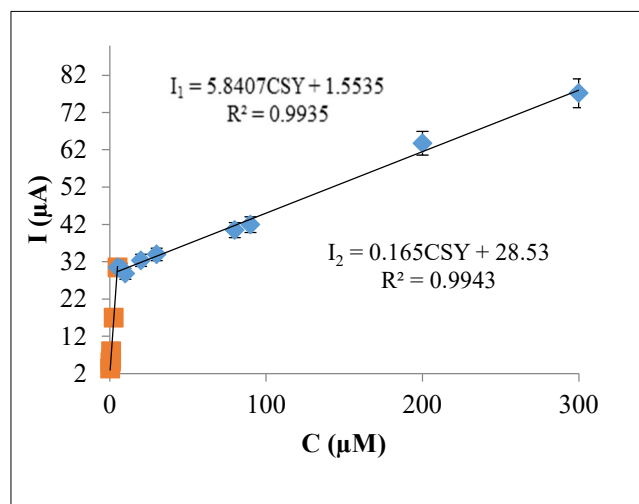


Fig. 10. Plot peak current vs. different concentrations of SY from 0.25 to 300 μM at PAP-OX/GCE in BRB of pH 9.0.

and stability of electrode modification. The study's sensor had a more extensive linear concentration range and greater stability and durability than some of the other sensors tested. In contrast to sensors discussed in earlier research, the electrode employed in this investigation offers advantages in terms of ease of fabrication, reduced time required for production, enhanced stability, and prolonged lifespan. Additionally, it has a quick and easy preparation process with low cost, making it more advantageous than almost all the other modified electrodes reported. Besides, the electrodes under examination exhibit a wider linear range compared to the electrodes previously discussed in the study. Based on these factors, the proposed sensor is beneficial for detecting SY in food samples in the presence of TZ. The modified electrode utilized in SY detection exhibits excellent analytical performance.

Selectivity Method

The selectivity of an analyte is a crucial factor that determines the accuracy of a method. To verify the method, this study examined 19 species that could coexist with food colors in actual samples and potentially affect peak current response. A solution containing 1 μM of SY was prepared in the supporting electrolyte in the presence of 2 μM of TZ, and varying concentrations of interfering species were added while SWASV was recorded. Results are presented in

Table 3. Comparison of the Analytical Performance of the Different Modified Electrodes for Determination of SY

Electrode	Technique	Modifier	Linear range (μM)	LOD (μM)	Lifetime	Ref.
CPE	CV and DPV	IL/NiFe ₂ O ₄ /rGO	0.05-5.0	0.03		[4]
CPE	SWV	Nd ₂ O ₃	2×10^{-3} - 2×10^{-1}	9×10^{-2}	5 Day	[52]
GCE	DPASV	ZnO/Cysteicacid nanocomposite	1×10^{-1} -3.0	3×10^{-2}		[53]
GCE	LSV	GO/MWCNTs nanocomposite	9×10^{-2} -8.0	25×10^{-3}		[10]
SPCEs	DPASV	rGO/NiBTC/SPCEs	5×10^{-2} -5.0	25×10^{-3}	7 Days	[54]
GC-RDE	DPASV	β -CD-PDDA-Gr composite	5×10^{-2} -20.0	125×10^{-5}	15 Days	[55]
Carbon-ceramic electrode	DPASV	IL/CCE	0.1-15.0	73×10^{-4}		[56]
CPE	SWASV	Silica impregnated with cetylpyridinium chloride	2×10^{-2} -1.0		7 Days	[57]
GCE	SWASV	Activated glassy carbon electrode (AGCE)	5×10^{-3} -1.0	17×10^{-4}		[58]
GCE	DPASV	CTABGO/MWNT/GCE	0.1 to 20.0	0.01	10 Cycle	[2]
GCE	SWASV	PAP-OX/GCE	25×10^{-2} -300.0	0.09	30 Day	This work

Table 4. Interference of some Foreign Species for a 1.0 μM Solution of SY in the Presence of 2 μM of TZ

Interfering species	Tolerance limit
Ascorbic acid, HPO ₄ , Co ²⁺ , Bi ³⁺	200
Na ⁺ , Cl ⁻ , Oleic acid	250
Hg ²⁺ , Cu ²⁺ , Cd ²⁺ , Mn ²⁺ , Ni ²⁺	300
Sucrose, Fe ²⁺	350
HCO ₃ ⁻	400
CaCl ₂ , Cu ²⁺	600
SO ₄ ⁻²	700
Glucose, Al ³⁺	1000

Table 4, with an error threshold of less than 5% being considered as the acceptable limit. Based on the data presented, the modified sensors exhibit good selectivity towards SY in the presence of interfering cations and anions.

Stability, Repeatability, and Reproducibility of the Modified Electrode

The modified electrode was used to draw the calibration

curve using several solutions with equal concentrations, the reproducibility of the modified electrode with PAP-OX was examined, and the standard deviation of the slopes was determined to be 1.14%, indicating excellent reproducibility. Three different modified electrodes were utilized to measure a series of solutions with the same concentration of SY in the presence of TZ, and their SWASV was recorded. The value of the relative standard deviation (% RSD) is calculated to be 4.09, suggesting that the modified electrode exhibits exceptional reproducibility. The stability of the electrode was assessed by generating a calibration curve and leaving the electrode in the laboratory for 30 days before drawing another calibration curve. The slopes of the two calibration curves were compared, and the findings indicated that the slope changes were below 0.5%, demonstrating that the electrode was stable.

Real Sample Analysis

In order to evaluate the suitability of the newly developed electrochemical sensor for detecting SY in food samples, a total of ten edible specimens, namely ice cream, Jelly powder, soft drink, fruit juice, pastille, chocolate stone, and smarties were examined using the designed electrode.

Subsequently, the food specimens were intentionally adulterated with different standard concentrations of SY. Subsequently, the SWASV peak current responses were measured consecutively. The results obtained have been presented in Table 5. The recovery values obtained from the analysis of the investigated samples demonstrate a consistent range of 95.9% to 104.1% across three successful

measurements. Furthermore, the relative standard deviation (%RSD) values for all samples demonstrated a level below 5% across three replications. Hence, it can be inferred that the developed sensor exhibits satisfactory performance in measuring SY in various real samples. Additionally, the presence of complex matrices in the specimens did not impact the analytical capabilities of the electrode.

Table 5. Determination of SY at Different Edible Specimens

Real samples	Measured (μM)	Added Amounts (μM)	Found Amounts (μM)	Recovery (%)
Ice cream 1	ND	0.316	0.312	98.8
		1.1	1.114	101.3
		1.63	1.62	99.4
Ice cream 2	ND	0.316	0.329	104.1
		1.1	1.07	97.3
		1.63	1.604	98.4
Jelly powder 1	0.474	0.790	1.253	99.1
		1.574	2.060	100.6
		2.104	2.544	98.7
Jelly powder 2	0.739	1.055	1.720	95.9
		1.839	2.539	98.5
		2.369	3.207	103.2
Soft drink 1	ND	0.316	0.314	99.5
		1.1	1.088	98.9
		1.63	1.658	101.7
Soft Drink 2	1.03	1.346	2.457	103.4
		2.13	3.1	98.09
		2.66	3.658	99.12
Fruit juice 1	0.880	1.196	2.011	96.9
		1.98	2.791	97.6
		2.51	3.421	100.9
Fruit juice 2	0.373	0.689	0.685	99.4
		1.789	1.769	98.9
		2.003	2.067	103.2
Pastille	0.611	0.927	1.532	99.6
		1.711	2.373	102.2
		2.241	2.826	99.1
Chocolate Stone	ND	0.316	0.329	104.1
		1.1	1.136	103.3
		1.63	1.628	99.9
Smarties	0.788	1.104	1.833	96.9
		1.888	2.625	98.1
		2.418	3.228	100.7

CONCLUSION

This study utilized a sensor to detect and measure SY in the presence of TZ in various food samples, including ice cream, jelly powder, pastille, chocolate, fruit juice, soft drinks, and smarties. SWASV parameters were screened using the Plackett-Burman design to achieve good analytical performance, with important factors such as pH, Number of cycles, step voltage, and precipitation potential selected. The BBD was utilized to optimize the screened parameters after their identification the sensor was discovered to have a linear range spanning 0.25 to 300 μ M. Furthermore, it presented good selectivity, stability, repeatability, and reproducibility the electrochemical method was effectively applied to measure SY in several food samples that also contained TZ. The recovery rate of the measured samples ranged from 95.9% to 104.1%.

REFERENCES

- [1] Y. Ou, X. Wang, K. Lai, Y. Huang, B.A. Rasco, Y. Fan, *J. Agric. Food Chem.* 66 (2018) 2954.
- [2] Y.J. Yang, W. Li, *Russ. J. Electrochem.* 51 (2015) 218.
- [3] S.-C. Sun, B.-C. Hsieh, M.-C. Chuang, *Electrochim. Acta* 319 (2019) 766.
- [4] R. Darabi, M. Shabani-Nooshabadi, *Food Chem.* 339 (2021) 127841.
- [5] K. Deng, Ch. Li, X. Li, H. Huang, *J. Electroanal. Chem.* 780 (2016) 296.
- [6] W. Zhang, T. Liu, X. Zheng, W. Huang, Ch. Wan, *Colloids Surf. B.* 74 (2009).
- [7] M. Wang, J. Zhao, *Sens. Actuators B Chem.* 216 (2015) 578.
- [8] Q.T. Tran, Th.T. Phung, Q.T. Nguyen, T. G.Le, C. Lagrost, *Anal. Bioanal. Chem.* 411 (2019) 7539.
- [9] S.M. Ghoreishi, M. Behpour, M. Golestaneh, *Food chem.* 132 (2012) 637.
- [10] X. Qiu, L. Lu, J. Leng, Y. Yu, W. Wang, M. Jiang, L. Bai. *Food Chem.* 190 (2016) 889.
- [11] D. Mishra, *Handbook of Oxidative Stress in Cancer: Mechanistic Aspects* (2020)1.
- [12] O.I. Lipskikh, E.I. Korotkova, Ye.P. Khristunova, J. Berek, B. Kratochvil, *Electrochim. Acta* 260 (2018) 974.
- [13] E.F.S. Authority, *EFSA Journal* 11 (2013) 3442.
- [14] E.P.o.F. Additives, N.S.a.t. Food, *EFSA Journal* 12 (2014) 3765.
- [15] C. Campanale, C. Massarelli, I. Savino, V. Locaputo, V.F. Uricchio, *Int. J. Environ. Res. Public Health*, 17 (2020) 1212.
- [16] F. Gosetti, V. Gianotti, S. Polati, M.C. Gennaro, *J. Chromatogr. A.* 1090 (2005) 107.
- [17] A.V. Jager, F.G. Tonin, M.F.M. Tavares, *J. Sep. Sci.* 28 (2005) 957.
- [18] N.E. Llamas, N. E. Llamas, M. Garrido, M.S. Di Nezio, B.S.F. Band, *Anal. Chim. Acta* 655 (2009) 38.
- [19] Y. Zhu, L. Zhang, L. Yang, *Mater. Res. Bull.* 63 (2015) 199.
- [20] X. Yang, N. Luo, Zh. Tan, Zh. Jia, X. Liao, *Food Anal. Methods* 10 (2017) 1308.
- [21] F. Pogacean, M. Coros, V. Mirel, L. Magerusan, L. Barbu-Tudoran, A. Vulpoi, R.-I.S.-van Staden, S. Pruneanu, *Microchem. J.* 147 (2019) 112.
- [22] P.-A. Kolozof, A.B. Florou, K. Spyrou, J. Hrbac, M. I. Prodromidis, *Sens. Actuators B Chem.* 304 (2020) 127268.
- [23] N.A. Kumar, H.-J. Choi, Y.R. Shin, D.W.Chang, L. Dai, J.-B. Baek. *ACS Nano.* 6 (2012) 1715.
- [24] J. Fei, K.G. Lim, G.T.R. Palmore, *Chem. Mater.* 20 (12) (2008) 3832.
- [25] J. Chen, Y. Zhu, J. Huang, J. Zhang, D. Pan, J. Zhou, J.E. Ryu, A. Umar, *Zh. Guo. Polym Rev (Phila Pa)*, 61 (2021) 157.
- [26] Y. Kim, *J. Photochem. Photobiol.* 204 (2009) 110.
- [27] J. Stejskal, M. Hajná, V.Kašpárková, P. Humpolíček, A. Zhigunov, M. Trchová, *Synth. Met.* 195 (2014) 286.
- [28] S.N. Vieira, L.F. Ferreira, D.L. Franco, A.S. Afonso, R.A. Gonçalves, A. G.Brito-Madurro, J.M. Madurro, *Macromol. Symp.* (2006). Wiley Online Library.
- [29] H.A. Menezes, G. Maia, *J. Electroanal. Chem.* 586 (2006) 39.
- [30] C. Wang, Zh. Xiong, P. Sun, R. Wang, X. Zhao, Q. Wang. *J. Electroanal. Chem.* 801 (2017) 395.
- [31] S.L.C. Ferreira, R.E. Bruns, H.S. Ferreira, G.D. Matos, J.M. David, G.C. Brandao, E.G.P. da Silva, L.A. Portugal, P.S. dos Reis, A.S. Souza, W.N.L. dos Santos. *Anal. Chim. Acta* 597 (2007) 179.

- [32] M. Ghani, S.M. Ghoreishi, Sh. Salehinia, N. Mousavi, H. Ansarinejad, *Microchem. J.* 146 (2019) 149.
- [33] M. Foroughi, A.R. Rahmani, Gh.Asgari, D. Nematollahi, K. Yetilmezsoy, M.R. Samarghandi, *Fresenius Environ. Bull.* 27 (2018) 1914.
- [34] Z. Doroudi, A. Niazi, *Pol. J. Chem. Technol.* 20 (2018) 21.
- [35] M. Chao, X. Ma, *Food Anal. Methods* 8 (2015) 130.
- [36] M. Wang, Y. Gao, Q. Sun, J. Zhao, *J. Electrochem. Soc.* 161 (2014) B297.
- [37] T. Gan, J. Sun, W. Meng, L. Song, Y. Zhang, *Food Chem.* 141 (2013) 3731.
- [38] Ç.C. Koçak, Z. Dursun, *J. Electroanal. Chem.* 694 (2013) 94.
- [39] L.F. Ferreira, J.F.C. Boodts, A.G. Brito-Madurro, J.M. Madurro, *Polym. Int.* 57 (2008) 644.
- [40] M.R. Jalali-Sarvestani, T. Madrakian, A. Afkhami, *Anal. Bioanal. Chem. Res.* 8 (2021) 245.
- [41] H.S. Magar, R.Y.A. Hassan, A. Mulchandani, *Sens.* 21 (2021) 6578.
- [42] Bard, *ELECTROCHEMICAL METHODS Fundamentals and Applications.* New York, NY, 1980.
- [43] S. Lanka, J.N.L. Latha, *Int. J. Biol. Chem.* 9 (2015) 207.
- [44] A. Haaland, *Angew. Chem., Int. Ed. Engl.* 28 (1989) 992.
- [45] S. Velayudam, K. Murugan, *South Indian J. Biol. Sci.* 1 (2015) 7.
- [46] K. Vanaja, R. Shobha Rani, *Clin. Res. Regul. Aff.* 24 (2007) 1.
- [47] M.R.J. Sarvestani, T. Madrakian, A. Afkhami, *Talanta* 250 (2022) 123716.
- [48] A. Joglekar, A. May, *CFW*, 32 (1987) 857.
- [49] S.H. Ahmadi, A. Manbohi, K.T. Heydar, *Anal. Chim. Acta.* 853 (2015) 335.
- [50] M. Gómez, V. Arancibia, C. Rojas, E. Nagles, *Int. J. Electrochem. Sci.* 7 (2012) 7493.
- [51] C.V. Moolya, N.P. Shetti, D.S. Nayak, *Mater. Today: Proc.* 18 (2019) 1116.
- [52] K. Marquez-Mariño, J. Penagos-Llanos, O. García-Beltrán, E. Nagles, J.J. Hurtado, *Electroanalysis.* 30 (2018) 2760.
- [53] P.S. Dorraji, F. Jalali, *Food Chem.* 227 (2017) 73.
- [54] J.-H. Wu, H.-L. Lee, *Microchem. J.* 158 (2020) 105133.
- [55] X. Ye, *Anal. Chim. Acta* 779 (2013) 22.
- [56] M.R. Majidi, M.H. Pournaghi-Azar, R.F. Bajeh Ba, A.H. Nasser, *Ionics* 21 (2015) 863.
- [57] A. Chebotarev, A. Koicheva, K. Bevziuk, K. pliuta, D.snigur, *J. Food Meas. Charact.* 13 (2019) 1964.
- [58] Y. Lu, Ch. Bao, J. Zou, J. Xiao, W. Zhong, Y. Gao, *Mol.* 27 (2022) 5221.